Development of Thyroid Model for ICRP Reference Pediatric Computational Phantoms

Chansoo Choi[a], Yeon Soo Yeom[b], Bangho Shin[a], Haegin Han[a], Sangseok Ha[a], Sungho Moon[a], Gahee Son[a], Chan Hyeong Kim[a*]

[a] *Department of Nuclear Engineering, Hanyang University, 222 Wangsimni-ro, Seongdong-gu, Seoul 04763, Korea*
[b] *National Cancer Institute, National Institute of Health, 9609 Medical Center Drive, Bethesda, MD 20850, USA*
[*] *Corresponding author: chkim@hanyang.ac.kr*

1. Introduction

Following the issuance of the 2007 Recommendations [1], the International Commission on Radiological Protection (ICRP) has released voxel-type reference computational phantoms (VRCPs) representing reference adult [2] and pediatric (newborn, 1, 5, 10, and 15 years) [3] males and females. The VRCPs has been used to produce reference dose coefficients (DCs) for various exposure scenarios considered in 2007-Recommendation-based ICRP dosimetry system. The VRCPs, however, have some limitations due to the geometric characteristics inherent in all the voxel-based phantoms, resulting in unreliable DCs for weakly-penetrating radiations.

To address the limitations of the VRCPs, ICRP Task Group 103 has been devoted to the development of the next-generation ICRP reference phantoms, mesh-type reference computational phantoms (MRCPs), which are the mesh counterparts of the VRCPs but represent more improved anatomical structures than the VRCPs. The task group completed the development of the adult MRCPs [4] and are currently developing the pediatric MRCPs. In this paper, we will report the thyroid model of the pediatric MRCPs, which is not only a radiosensitive target organ required for effective dose calculation but also an important source organ especially for internal exposures to radioactive iodine, explaining the development process and their dosimetric impact.

2. Materials and Methods

The pediatric MRCPs' thyroid models were constructed based on those of the pediatric VRCPs but their shapes and positions were anatomically improved to represent the typical features of the pediatric population. For this, first, the primary thyroid models were produced using both the pediatric VRCPs [3] through conversion and rendering procedures following the methods used in the previous study [5]. Then, the primary thyroid models were modified according to the data of the isthmus thickness, width, and height, which were determined from relevant scientific literature and measurement data [6–12]. Finally, the thyroid models were installed in their proper positions, that is, in front of the second and third tracheal cartilage (i.e., top end region of the trachea) [13], matching the target depth beneath the skin surface [14].

The developed thyroid models, along with other organs that had been previously constructed, were implemented in Geant4 Monte Carlo radiation transport code (version 10.06) to calculate the photon specific absorbed fractions (SAFs) for internal exposures for the thyroid as a source region and oesophagus wall as a target region, as examples. For the comparison, the pediatric VRCPs were also implemented in Geant4 code and used to calculate the SAFs for the same exposure cases. Primary particle energies ranging from 10 keV to 10 MeV were considered and the physics library of *G4EMLiverMorePhysics* was used. The statistical errors for the DCs and SAFs were less than 5%.

3. Results and Discussion

Figure 1 shows the thyroid model of the 1-year-old female MRCP, along with that of the 1-year-old female VRCP, as representative of the thyroid models of the pediatric MRCPs. It can be seen that the anatomical features of the thyroid model of the MRCP, especially the position and depth beneath the skin surface, are significantly different compared to that of the VRCP. For other phantoms, it was observed that there are significant anatomical differences, although not as markedly as the 1-year-old phantoms. The dimensions of the thyroid models (i.e., isthmus thickness, width, and height and depth beneath the skin surface) are in accordance with the target values within 5% of deviation.

Figure 2 compares the SAFs of the pediatric MRCPs and VRCPs calculated for the thyroid as a source region and the oesophagus as a target region for photons. Note

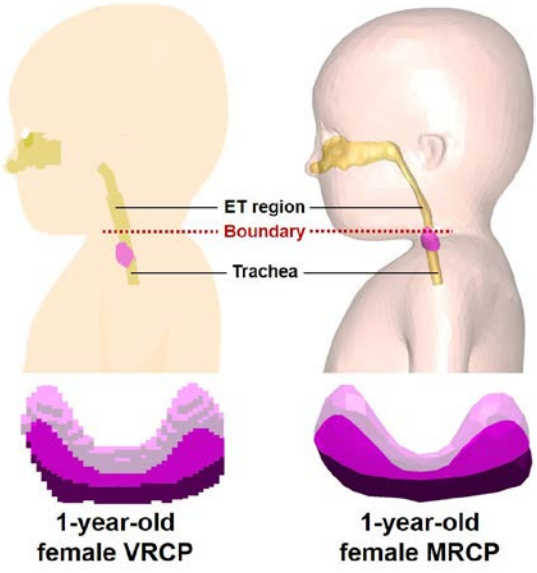

Figure 1. Developed thyroid model of the 1-year-old female VRCP (left) and MRCP (right).

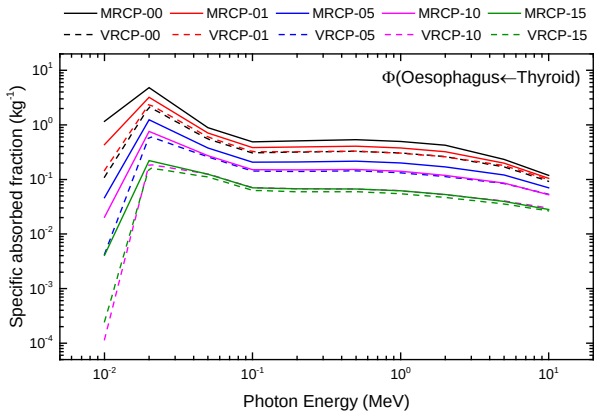

Figure 2. Photon SAFs for the thyroid as a source region and the oesophagus as a target region. Each SAF was averaged over sex.

that each SAF was averaged over sex. For all ages, large differences were observed over the entire energy range. Especially at low energies (<0.02 MeV), much larger differences were observed, the maximum difference being ~170 times for 10 years at 0.01 MeV. The SAFs of the MRCPs tend to decrease as age increases, while those of the VRCPs show no tendency. Considering that (1) the distance between the thyroid and oesophagus increases and (2) the oesophagus mass increases as age increases, the results indicate that the MRCPs provide more reliable SAFs for the cases considered in the present study.

4. Conclusion

In the present study, we developed the newborn, 1-, 5-, 10-, and 15-year-old male and female thyroid models of the pediatric MRCPs, which represent the typical features of the pediatric population. Then, the photon SAFs for some internal exposure cases (source: thyroid and target: oesophagus) were calculated, which were then compared with those calculated with the pediatric VRCPs. The comparison results showed that there were large differences in the SAFs especially at low energies. Considering anatomical improvements and reasonable tendency of the SAFs with age, we believe the pediatric MRCPs will provide more reliable dose values in other exposure cases where the thyroid is considered as a source and/or target regions.

REFERENCES

[1] ICRP, The 2007 recommendations of the International Commission on Radiological Protection, ICRP Publication 103, Ann. ICRP 32 (2–4), 2007.
[2] ICRP, Adult reference computational phantoms, ICRP Publication 110, Ann. ICRP 39 (2), 2009.
[3] ICRP, Paediatric reference computational phantoms, ICRP Publication 143, Ann. ICRP 49 (1), 2020.
[4] ICRP, Adult mesh-type reference computational phantoms, ICRP Publication 145, Ann. ICRP 49 (3), 2020.
[5] C. Choi, B. Shin, Y.S. Yeom, et al., Development of skeletal systems for ICRP pediatric mesh-type reference computational phantoms, J. Radiol. Prot., 2021, in press, doi: 10.1088/1361-6498/abd88d.
[6] J.H. Sea, H. Ji, S.K. You, et al., Age-dependent reference values of the thyroid gland in pediatric population; from routine computed tomography data, Clin. Imag., Vol. 56, pp. 88–92, 2019.
[7] G. Ozguner, O. Sulak, Size and location of thyroid gland in the fetal period, Surg. Radiol. Anat., Vol. 36, pp. 359–367, 2014.
[8] E.C.K. Tong, S. Rubenfeld, Scan measurements of normal and enlarged thyroid gland, Am. J. Roentgenol. Radium Ther. Nucl. Med., Vol. 115, pp. 706–708, 1972.
[9] A. Harjeet, D. Sahni, I. Jit, et al., Shape, measurements and weight of the thyroid gland in northwest Indians, Surg. Radio. Anat., Vol. 26, pp. 91–95, 2004.
[10] S.D. Joshi, S.S. Joshi, S.R. Daimi, et al., The thyroid gland and its variations: a cadaveric study, Folia Morphol., Vol. 69, pp. 47–50, 2010.
[11] Z. Ozgur, S. Celik, F. Govsa, et al., Anatomical and surgical aspects of the lobes of the thyroid glands, Eur. Arch. Otorhinolaryngol., Vol. 268, pp. 1357–1363, 2011.
[12] H.S. Won, S.H. Han, C.S. Oh, et al., The location and morphometry of the thyroid isthmus in adult Korean cadavers, Anat. Sci. Int., Vol. 88, pp. 212–216, 2013.
[13] H. Ellis, Anatomy of the thyroid and parathyroid glands, Surgery (Oxford), Vol. 25, 467–468, 2007.
[14] I.A. Likhtarev, G.M. Gulko, B.G. Sobolev, et al., Evaluation of the 131I thyroid-monitoring measurements performed in Ukraine during May and June of 1986, Health Physics., Vol. 69, pp. 6–15, 1995.